NEW FLUORENE MOLECULES WITH EFFICIENT TWO-PHOTON ABSORPTION FOR MULTIDISCIPLINARY NONLINEAR OPTICAL APPLICATIONS

M.V. BONDAR, O.V. PRZHONSKA, C.O. YANEZ[1], K.D. BELFIELD[1]

UDC 539.2;535.3

Institute of Physics, Nat. Acad. of Sci. of Ukraine
(46, Nauky Prosp., Kyiv 03028),

[1]**Department of Chemistry and CREOL, The College of Optics and Photonics, University of Central Florida**
(Orlando, FL 32816-2366, USA)

Linear photophysical and two-photon absorption (2PA) properties of new sulfur-containing fluorene compounds, 2,7-bis(4-(phenylthio)styryl)-9,9-didecyl-9H-fluorene (**1**) and 2,7-bis(4-(phenylsulfonyl)styryl)-9,9-didecyl-9H-fluorene (**2**), are investigated with respect to a broad variety of nonlinear optical applications, including multiphoton fluorescence and lifetime bioimaging. The high fluorescence quantum yield and the effect of excited state symmetry breaking are observed. The 2PA spectra were measured over a broad spectral range 480–880 nm by the two-photon fluorescence and *Z*-scan techniques. The 2PA cross sections (up to 2000 GM) are calculated using a numerical fitting algorithm taking the excited state absorption and stimulated emission processes into account.

1. Introduction

The synthesis and nonlinear optical properties of new fluorene-based compounds remain a subject of intense scientific research due to multidisciplinary nonlinear optical applications such as two-photon power limiting, organic light emitting diodes, two-photon microfibrication, optical data storage, photodynamic cancer therapy, etc. [1–10]. Fluorene molecules with high fluorescence quantum yield, Φ, large 2PA cross sections, $\delta_{2\mathrm{PA}}$, and a broad range of fluorescence lifetimes, τ, are promising compounds for the successful application in multiphoton fluorescence and lifetime imaging microscopy [1,2]. The well-known fluorescence labels such as green fluorescent proteins [11], plant-derived phytofluors [12], phycobiliproteins [13], and others are not optimized for 2PA. They exhibit relatively low values of $\delta_{2\mathrm{PA}}$ and thus the corresponding action cross sections, $\Phi \times \delta_{2\mathrm{PA}}$, that are crucial for this type of applications. Therefore, even though many optical properties of fluorenes, including two- and three-photon absorption, have been recently reported (see, e.g., [4,14–17]), much more remains to be understood.

The unsubstituted fluorene molecule presented in Fig. 1 (top) is a rigid flat system which is characterized by the strong π molecular orbital overlap between the rings, providing complete π electron delocalization. Importantly that fluorene can be easily functionalized in positions 2, 4, 7, and 9 (see Fig. 1) facilitating the development of a broad variety of fluorene-based structures with specific nonlinear optical properties. Reactive positions 2, 4, and 7 have been used to extend the conjugation length crucial for optical nonlinearity. Reactive position 9 facilitates the introduction of solubilizing groups such as alkyl chains or, in the case of biological probes, more hydrophilic groups such as ethylene-oxy moieties. Based on the peculiarities of the electronic distribution, fluorene molecules can be presented as symmetric D-π-D, A-π-A or asymmetric D-π-A structures, where D and A refer to electron donor and electron acceptor, respectively.

In this paper, the linear photophysical properties, including excitation anisotropy, fluorescence lifetimes, and 2PA spectra of new sulfur-containing fluorene derivatives, 2,7-bis(4-(phenylthio)styryl)-9,9-didecyl-

9H-fluorene (**1**) and 2,7-bis(4-(phenylsulfonyl)styryl)-9,9-didecyl-9H-fluorene (**2**), have been investigated in comparison to the well-known symmetric fluorenes **3** (D-π-D) and **4** (A-π-A) [18] shown in Fig. 1. The electronic structures of **1** and **2** can be described as quadrupolar-type arrangements A-π-D-π-A (**1**) and D-π-D-π-D (**2**), which is highly desirable for increasing δ_{2PA}. The introduction of oxygen atoms in compound **2** changes the nature of the electronic distribution and dramatically increases the photooxidation resistance. Fluorenes **1** and **2** with a highly fluorescent core contain a sufficiently large number of π electrons and, therefore, are expected to have potential for different nonlinear optical applications, especially for 2PA and bioimaging [19,20]. Moreover, sulfur-containing molecules exhibit good labeling abilities for the visualization of biological processes in living tissue, for example, for imaging of a serotonin transporter in a living human brain as shown in [21].

The goal of this paper is the comprehensive linear and nonlinear optical investigations of new fluorene molecules **1** and **2** potentially efficient for the development of new two-photon fluorescence bioprobes with high fluorescence quantum yields, increased 2PA cross sections, and high photochemical stability. In spite of a large number of publications reporting data on 2PA, it is still challenging to obtain the reliable 2PA spectra of organic compounds. In this paper, two different methods were employed for these investigations in order to increase the reliability of results. The first is the relative two-photon fluorescence (2PF) method introduced by Galanin et al. in 1966 [22] and comprehensively developed by Webb et al. in 1996 [23]. The second method is the well-known open aperture Z-scan technique introduced by Van Stryland et al. in 1990 [24]. The last method was used in conjunction with a modified numerical fitting algorithm, taking the possible excited state absorption (ESA) and stimulated emission processes into account [18].

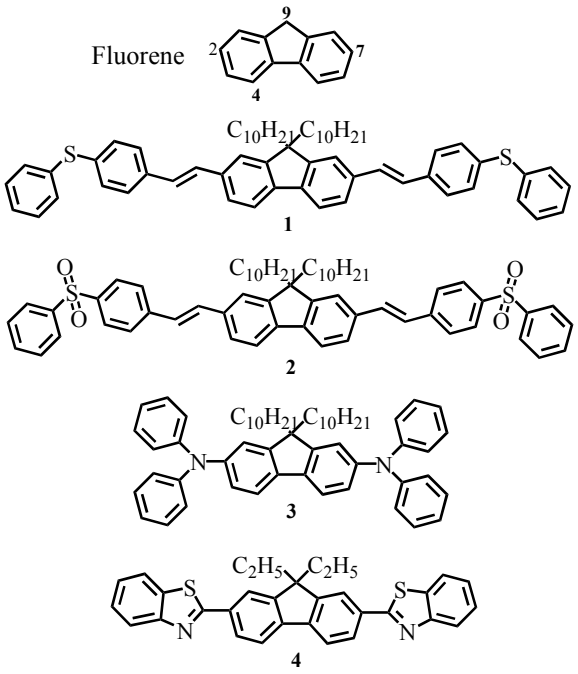

Fig. 1. Chemical structures of unsubstituted fluorene (top), fluorene-based sulfur-containing compounds **1** and **2;** 9,9-didecyl-2,7-bis-(N,N-diphenylamino)fluorene (**3**) and 9,9-diethyl-2,7-bis-(N,N-benzothiazoyl)fluorene (**4**)

2. Experimental

2.1. Materials and linear photophysical characterization

The synthesis of new fluorene derivatives **1** and **2** will be described elsewhere. The absorption spectra were measured with an Agilent 8453 UV–Visible spectrophotometer in spectroscopic grade solvents hexane, tetrahydrofuran (THF), polytetrahydrofuran (pTHF), and toluene. No concentration dependences were observed in the range of concentrations 10^{-6} M-10^{-2} M, indicating the negligible amount of aggregated molecules in the solutions. The steady-state fluorescence and excitation anisotropy spectra were recorded with a PTI QuantaMaster spectrofluorimeter for concentrations $\leq 10^{-6}$ M. All fluorescence spectra were corrected with the spectral responsivity of a PTI detection system. The excitation anisotropy spectra were obtained by the standard method [25] in viscous pTHF ($\sim$ 200 cP at 300 K) to determine the fundamental values of molecular anisotropies $r_0 = (3\cos^2\alpha - 1)/5$ (α is the angle between the absorption and emission transition dipoles), which can be reached in the case $\tau \ll \theta = \eta V/kT$, where θ is the rotational correlation time; η, V, k, and T are the solvent viscosity, volume of the rotating molecule, Boltzmann's constant, and temperature, respectively. Fluorescence quantum yields Φ were determined by a relative method with 9,10-diphenylanthracene in cyclohexane as a standard (Φ = 0.95) [25]. The values of lifetimes τ were obtained by a time-correlated single photon counting system PicoHarp300 with a time resolution of $\approx$80 ps using the linear polarized femtosecond excitation oriented by a magic angle.

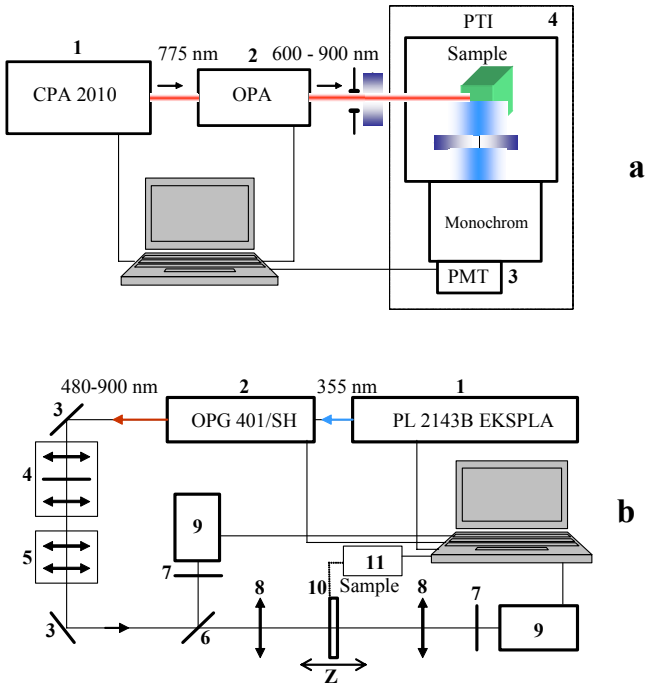

Fig. 2. Experimental setups for 2PA measurements. (**a**) 2PF method: femtosecond laser (*1*); optical parametric amplifier (*2*); photomultiplier (*3*); PTI QuantaMaster spectrofluorimeter (*4*). (**b**) open aperture Z-scan method: picosecond laser (*1*); optical parametric generator (*2*); 100% reflection mirrors (*3*); space filter (*4*); telescope (*5*); beam splitter (*6*); filters (*7*); focusing lens (25 cm); *9* – silicon detectors (*9*); 1-mm cuvette (*10*); step motor (*11*)

2.2. 2PA Measurements

The 2PA spectra were measured over a broad spectral region 480–880 nm by two separate methods: 2PF [23] and open aperture Z-scan [24]. The relative 2PF technique shown in Fig. 2,*a* was used with a PTI QuantaMaster spectrofluorimeter coupled with a femtosecond Clark-MXR CPA-2010 laser that pumped optical parametric generator/amplifiers (TOPAS) with the tuning range 600–900 nm, pulse duration ≈ 140 fs (FWHM), 1-kHz repetition rate, and pulse energies of 0.05–0.15 μJ. Rhodamine B in methanol ($\Phi = 0.7$) and Fluorescein in water ($\Phi = 0.9$ at pH=11) were used as 2PA standards. The values of $\delta_{2\mathrm{PA}}$ were determined by the equation [23]

$$\delta^S_{2\mathrm{PA}} = \delta^R_{2\mathrm{PA}} \frac{\langle F(t)\rangle_S N_R \Phi_R \varphi_R \langle P(t)\rangle^2_R}{\langle F(t)\rangle_R N_S \Phi_S \varphi_S \langle P(t)\rangle^2_S}, \qquad (1)$$

where $\langle F(t)\rangle$, $\langle P(t)\rangle$, N, and φ are the averaged fluorescence intensity, excitation power, molecular concentration, and geometric factor, respectively. Subscripts S and R refer to the sample and reference. Special attention was paid to verify the independence of the fluorescence quantum yield of the excitation wavelength λ_{exc} and the quadratic dependence of the 2PF intensity on the excitation power.

Another method used in 2PA cross section measurements was an open aperture Z-scan shown in Fig. 2,*b*. In these measurements, a picosecond Nd:YAG laser (PL 2143 B Ekspla) with a repetition rate of 10 Hz coupled to an optical parametric generator (OPG 401/SH) with the tuning range 480–880 nm, pulse duration of ≈35 ps (FWHM), and pulse energies of 0.05–5 μJ was used. As was shown in [18], picosecond lasers with relatively high pulse energy can afford reliable 2PA data, when ESA and stimulated emission processes are taken into account. In the case of degenerate 2PA and for spatially and temporally Gaussian beam profiles, the values of time integrated energy transmittance can be analytically expressed as [24]

$$T(z) = \frac{1}{\sqrt{\pi}\beta I_0(z) L} \int\limits_{-\infty}^{+\infty} \ln[1 + \beta I_0(z) L \exp(-t'^2)] dt', \qquad (2)$$

where β is the 2PA coefficient; z and L are the longitudinal space coordinate and the sample length, respectively; $I_0(z) = \frac{2E_P}{\pi^{3/2}\omega(z)^2\tau_P}$, where E_P is the pulse energy, $\omega(z)$ is a transverse size of the beam (HW1/e^{2}M), and τ_P is the pulse duration (HW1/eM). The values of $\delta_{2\mathrm{PA}}$ can be calculated through β as $\delta_{2\mathrm{PA}} = \beta \frac{h\nu}{N}$ (where $h\nu$ is the photon energy) by fitting the experimental data with Eq. (2). It should be noted that Eq. (2) is based on the thin sample approximation, predominance of the ground state population over the excited state one, and the absence of ESA and stimulated emission processes. However, for many molecules, the ESA contribution cannot be neglected. Therefore, in this work, a modified fitting procedure developed in [18] was used:

$$T(z)_{\mathrm{Mod}} = \frac{4}{\sqrt{\pi}\omega(z)^2\tau_P} \int\limits_r \int\limits_t \exp[-2r^2/\omega(z)^2 - t^2/\tau_P^2] \times$$

$$\times [1 - k(z, r, t) L] r dr dt, \qquad (3)$$

where $T(z)_{\mathrm{Mod}}$ is the modified transmittance, $k(z, r, t)$ is the nonlinear absorption coefficient (r – transverse coordinate) numerically calculated from the state

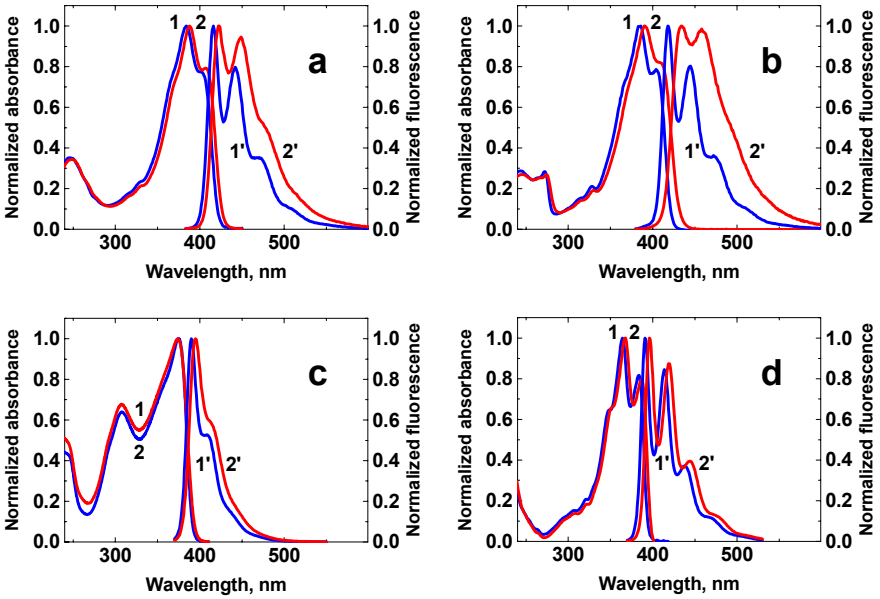

Fig. 3. Normalized absorption (*1* and *2*) and fluorescence (*1′*, *2′*) spectra of fluorenes **1** (*a*), **2** (*b*), **3** (*c*) and **4** (*d*) in hexane (*1*, *1′*, online blue color) and THF (*2*, *2′*, online red color)

populations $N_i(z, r, t)$ taking ESA and stimulated emission processes into account. The values of δ_{2PA} were determined from the simultaneous fitting of 2–3 experimental Z-scan curves.

3. Results and Discussion

3.1. Linear spectral properties

The linear absorption, fluorescence, and excitation anisotropy spectra of fluorene compounds **1**–**4** are presented in Figs. 3–4, and the main parameters are summarized in Table 1. All absorption spectra were nearly independent of the solvent polarity. Weak vibrational modes (∼1300 cm^{-1}) corresponding to C–C skeleton vibrations were observed for more rigid fluorene **4** (Fig. 3,*d*, curves *1* and *2*). In contrast, the absorption spectrum of **3** is structureless, by indicating a nonplanar molecular geometry with the reduced electron-vibrational interaction. Weak vibrational shoulders are seen for new sulfur-containing fluorenes **1**–**2** (Fig. 3,*a,b*, curves *1* and *2*).

In contrast to absorption, the fluorescence spectra are solvent-dependent. For symmetric compounds **3** (type D-π-D) and **4** (A-π-A), the fluorescence spectra revealed a weak dependence on the solvent polarity, whereas compounds **1** (A-π-D-π-A) and **2** (D-π-D-π-D) exhibited a much stronger solvent dependence and more noticeable changes in the shape of fluorescence bands. The solvatochromic behavior of **1**–**2** can be described by the excited state (S_1) symmetry breaking phenomenon. According to the approach developed in [26], symmetric quadrupolar-type fluorene molecules can possess a double minimum on the excited state energy surface. In this case, the symmetric electronic distribution in S_1 becomes unstable, and the molecule relaxes to the potential minima corresponding to an asymmetric electronic distribution.

The dependences of the fluorescence quantum yield Φ on λ_{exc} for **1**–**2** and their fluorescence decay curves are presented in Fig. 4. It is seen that the values of Φ are high (≈ 1.0) and independent of λ_{exc}. The fluorescence decay curves exhibited the one-exponential decay with $\tau \sim$ 0.6–0.8 ns, indicative of the relatively fast spontaneous relaxation with the velocity $1/\tau_n = \Phi/\tau \approx (1.3{-}1.7)\cdot 10^9$ s^{-1}, where τ_n is the natural lifetime. These lifetimes were calculated by the Birks–Dyson equation [25]

$$1/\tau_n = 2880(g_1/g_2)(n_f^3/n_a)\frac{\int F(\nu)d\nu}{\int [F(\nu)/\nu^3]d\nu}\int [\varepsilon(\nu)/\nu]d\nu, \quad (4)$$

where g_1 and g_2 are the multiplicities of the ground and excited states (for singlet states, $g_1/g_2 = 1$); n_f and n_a are the refractive indices of the solvent; $\varepsilon(\nu)$ is the curve of the molecular extinction coefficient plotted in wavenumbers ν (μm^{-1}); and $F(\nu)$ is the quantum fluorescence intensity. The comparison of the

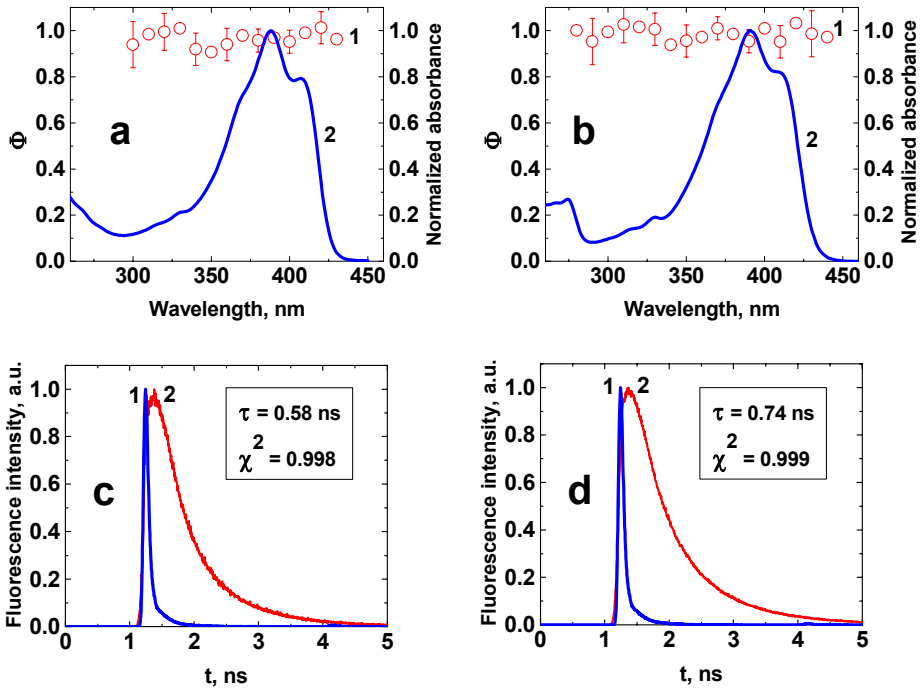

Fig. 4. Normalized absorption spectra (2*a,b* – online blue color) and the dependences of the fluorescence quantum yield Φ on λ_{exc}(1,*a,b* – online red color) for fluorenes **1** (*a*) and **2** (*b*). Instrument response function (1,*c,d* – online blue color) and fluorescence decays (*2*, online red color) for **1** (*c*) and **2** (*d*). All in THF

experimental τ and calculated lifetimes $\tau^{cal} = \tau_n \times \Phi$ revealed a noticeable deviation for compounds **1**–**2** in contrast to **3**–**4** with less pronounced disagreement (Table 1). These deviations for **1**–**2** correspond to the assumption of the excited state symmetry breaking effect.

T a b l e 1. Photophysical parameters of fluorenes 1 –4 in hexane (Hex), toluene (Tol), and THF: $\lambda_{ab}^{max}$and λ_{fl}^{max} – absorption and fluorescence peaks; ε^{max} – max extinction coefficients; Φ – fluorescence quantum yields, τ, τ^{cal} and τ_n – experimental, calculated, and natural lifetimes; r – anisotropy values in the main absorption bands

Compound	**1**		**2**			**3**		**4**	
Solvent	Hex	THF	Hex	Tol	THF	Hex	THF	Hex	THF
λ_{ab}^{max}, nm	384 ±1	388 ±1	384 ±1	391 ±1	391 ±1	375 ±1	374 ±1	364 ±1	367 ±1
λ_{fl}^{max}, nm	416 ±1	423 ±1	418 ±1	428 ±1	434 ±1	390 ±1	395 ±1	391 ±1	396 ±1
$\varepsilon^{max} \times 10^{-3}$, $M^{-1}\cdot cm^{-1}$	97 ±10	95 ±10	110 ±10	95 ±10	92 ±10	44 ±5	37 ±5	75 ±8	66 ±7
Φ	1.0 ±0.05	1.0 ±0.05	1.0 ±0.05	1.0 ±0.05	1.0 ±0.05	0.4 ±0.03	0.5 ±0.03	0.95 ±0.05	0.96 ±0.05
τ, ns	0.59 ±0.08	0.58 ±0.08	0.59 ±0.08	0.85 ±0.08	0.74 ±0.08	0.95 ±0.08	1.0 ±0.08	0.78 ±0.08	0.90 ±0.08
τ^{cal}, ns	1.03 ±0.1	1.08 ±0.1	1.0 ±0.1	1.0 ±0.1	1.17 ±0.1	0.84 ±0.3	1.15 ±0.3	1.14 ±0.15	1.25 ±0.15
τ_n, ns	1.03 ±0.1	1.08 ±0.1	1.0 ±0.1	1.0 ±0.1	1.17 ±0.1	2.1 ±0.2	2.3 ±0.2	1.2 ±0.15	1.3 ±0.15
r	0.083 ±0.01	0.102 ±0.01	0.081 ±0.01	0.125 ±0.01	0.093 ±0.01	0.042 ±0.01	0.049 ±0.01	0.040 ±0.01	0.063 ±0.01

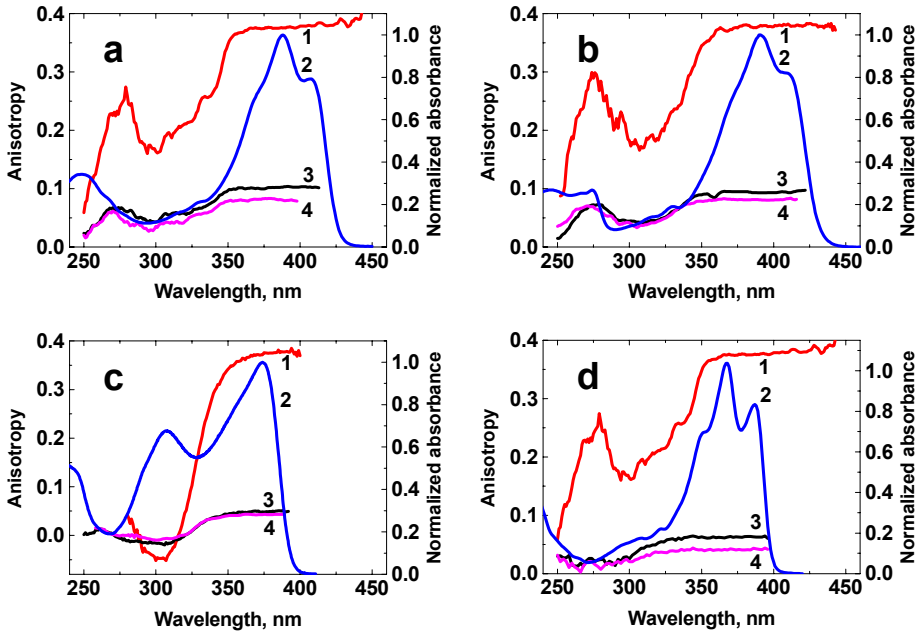

Fig. 5. Normalized linear absorption (*2* – online blue color) and the excitation anisotropy spectra in pTHF (*1* – online red color), THF (*3* – online black color), and hexane (*4* – online pink color) for fluorenes **1** (*a*), **2** (*b*), **3** (*c*) and **4** (*d*)

The excitation anisotropy spectra of fluorenes **1**–**4** (Fig. 5, curves *1, 3–4*) revealed the nature of the one-photon absorption bands. The constant values of anisotropies indicate that a single electronic transition is primarily responsible for the one-photon absorption at $\lambda_{exc} \geq 360$ nm. In low-viscosity solvents (hexane, THF, toluene, etc.), the anisotropy values decreased due to a rotational movement of the molecule in accordance with $r = r_0/(1 + \tau/\theta)$ [25]. The lowest value of r was observed in hexane. In viscous pTHF, the fluorescence lifetime $\tau \ll \theta$ ($\theta \geq 10$ ns at 300 K), and the excitation anisotropy reached its maximum value $r \approx r_0 \approx 0.38$ close to the theoretical limit of 0.4, reflecting the nearly parallel orientation of the absorption and emission dipoles. In this case, it is possible to determine the mutual orientation of the ground $S_0{-}S_1$ and excited $S_0{-}Sn$ transitions, which is important for the 2PA analysis. The decrease of the anisotropy at $\lambda_{exc} < 360$ nm and the following extremes correspond to the spectral positions of $S_0{-}Sn$ bands. For compounds **1**, **2**, and **4**, the anisotropy values are 0.15–0.3 in the region 270–340 nm (Fig. 5,*a,b,d*, curves *1*) corresponding to a range of angles 25°–40° between overlapped S_0 – Sn transitions. Note that these bands are sufficiently weak and cannot be resolved in the linear absorption spectra. In contrast, fluorene **3** exhibits an anisotropy minimum at ∼305 nm (Fig. 5,*c*, curve *1*) indicating to a well-separated transition attributed to diphenylamino terminal substituents [27]. A negative anisotropy value, $r_0 \approx -0.047$ at 305 nm, reflects the ≈ 60°-angle of this transition relative to the $S_0{-}S_1$ transition dipole.

3.2. 2PA efficiency of the investigated fluorenes

The 2PA spectra of compounds **1**–**4** obtained by the 2PF and *Z*-scan methods, along with their linear absorption spectra, are presented in Fig. 6. The results of two separate methods are in a good agreement and revealed relatively high δ_{2PA} values for the new sulfur-containing fluorenes **1**–**2** up to 2000 GM at $\lambda_{exc} \sim$ 650-680 nm. It was found that the 2PA spectra are nearly independent of the solvent polarity. The electronic nature of terminal substituents (donor or acceptor) did not play an essential role for **1**–**2** in contrast to **3**–**4,** where A-π-A-type molecules exhibited a noticeably higher δ_{2PA} values than those for D-π-D-type molecules. The 2PA spectra for fluorenes **1**–**2** represent the solitary bands with shoulders within $S_0{-}S_1$ with acceptably high δ_{2PA}=100–700 GM, overlapping nicely with the tuning range of commercial Ti:Saphire femtosecond lasers typically used for multiphoton microscopy. In contrast, fluorenes **3**–**4** possess much smaller $\delta_{2PA} < 50$ GM within the main absorption band. The decrease in δ_{2PA} at $\lambda_{exc} > 700$ nm was expected for the symmetric molecules in accordance

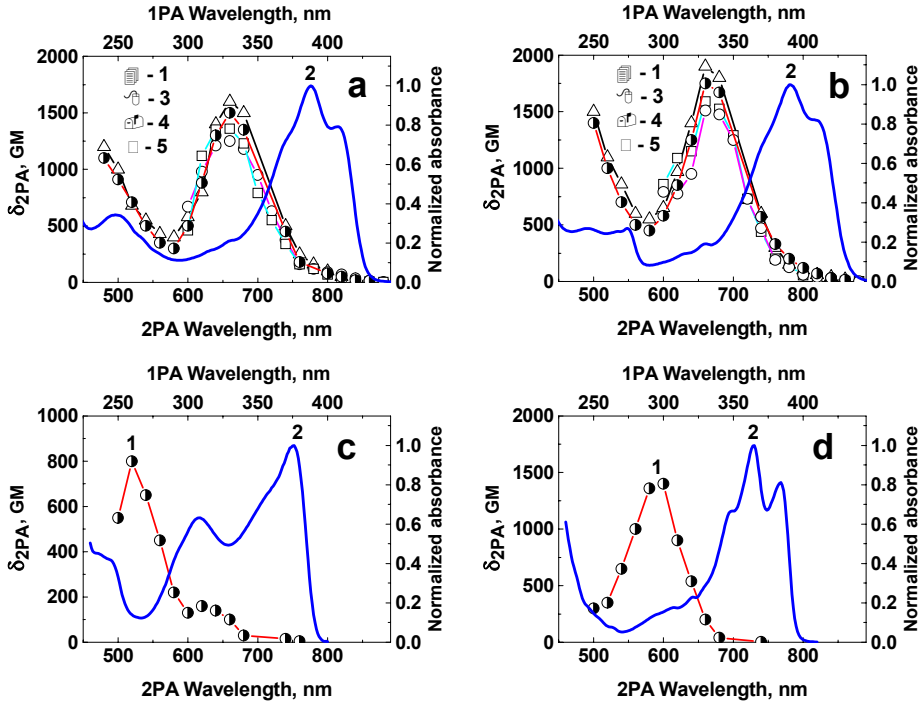

Fig. 6. Normalized one-photon absorption (1PA, right and top axes) spectra (*2* – online blue color) and 2PA spectra (left and bottom axes) in hexane (*1*, *4*) and THF (*2*, *3*, *5*), obtained by the *Z*-scan (*1*, *3*) and 2PF (*4*, *5*) methods for fluorenes **1** (*a*), **2** (*b*), **3** (*c*) and **4** (*d*)). Experimental errors of δ_{2PA} are ±20 %

with the 2PA selection rules [28]. However, fluorenes **1**–**4** are not centrosymmetric structures, and two-photon transitions are not strictly forbidden.

An increase of δ_{2PA} at $\lambda_{exc} < 580$ nm is presumably associated with the intermediate state resonant enhancement due to a decrease in the detuning energy $E = hc(1/\lambda_{ab}^{max} - 1/\lambda_{exc})$ [29]. It is known that the degenerate δ_{2PA} for a simplified 3-level model can be expressed by the following relation based on the sum-over-states approach [30, 31]:

$$\delta_{2PA} = \frac{64\pi^4}{15c^2h^2n^2}\left[\frac{\nu_{exc}^2 \left|\boldsymbol{\mu_{01}}\right|^2 \left|\boldsymbol{\mu_{1f}}\right|^2}{E^2+\Gamma_{01}^2}(1+2\cos^2\alpha_1)+\right.$$

$$\left.+\left|\Delta\boldsymbol{\mu_{01}}\right|^2 \left|\boldsymbol{\mu_{01}}\right|^2 (1+2\cos^2\alpha_2)\right] g'(\nu_{exc}), \qquad (5)$$

where $\nu_{exc} = c/\lambda_{exc}$; $\boldsymbol{\mu_{01}}$ and $\boldsymbol{\mu_{1f}}$ are the transition dipole moments for S_0–S_1 and S_1–S_f transitions (estimated by quantum-chemical calculations using Gaussian 03 [32]); $\Delta\boldsymbol{\mu_{01}} = \boldsymbol{\mu_0} - \boldsymbol{\mu_1}$ is the difference of the permanent dipole moments of S_0 and S_1; Γ_{01} is a damping constant; α_1 and α_2 are the angles between the vectors $\boldsymbol{\mu_{01}}$, μ_{1f} and $\Delta\boldsymbol{\mu_{01}}$, $\boldsymbol{\mu_{01}}$; $g'(\nu_{exc})$ is the normalized Lorentzian shape function. The calculated δ_{2PA} are in a good agreement with the experimental values for all fluorene molecules.

4. Conclusions

The linear photophysical and 2PA properties of new sulfur-containing symmetric fluorenes **1**–**2** have been investigated in comparison to the known structures **3**–**4** with diphenylamino and benzothiazolyl substituents. The high fluorescence quantum yields of **1**–**2** (≈ 1.0) are found to be independent of excitation wavelengths and solvent properties. The strong solvatochromic behavior of their fluorescence spectra is shown and explained by the excited state symmetry breaking effect.

The 2PA spectra are obtained by the 2PF and open aperture *Z*-scan methods with a modified fitting algorithm considering ESA and stimulated emission processes. The two-photon allowed absorption bands for **1**–**2** are observed at λ_{exc} ∼660 nm with the maximum cross sections up to 2000 GM. Relatively large δ_{2PA}, high fluorescence quantum yields, and photochemical stability make these compounds particularly attractive for a variety of nonlinear optical applications including

2PA data storage, fluorescence and lifetime bioimaging microscopy.

We wish to acknowledge the Civilian Research and Development Foundation (UKB2-2923-KV-07), the Ministry of Education and Science of Ukraine (grant M/49-2008), the National Science Foundation (grants ECS-0524533 and ECS-0621715), and the University of Central Florida Presidential Initiative for Major Research Equipment for the partial support of this work.

1. K.J. Schafer, S. Yao, K.D. Belfield *et al.*, Proc. SPIE **5329**, 201 (2004).
2. Z.-L. Huang and K.D. Belfield, Polymer Preprints (Amer. Chem. Soc., Division of Polymer Chemistry) **48**, 494 (2007).
3. M. Charlot, N. Izard, O. Mongin *et al.*, Chem. Phys. Lett. **417**, 297 (2006).
4. T.-C. Lin, G.S. He, Q. Zheng *et al.*, J. Mater. Chem. **16**, 2490 (2006).
5. L. Feng, C. Zhang, H. Bie *et al.*, Dyes and Pigments **64**, 31 (2005).
6. S. Tao, Z. Peng, X. Zhang *et al.*, Adv. Funct. Mater. **15**, 1716 (2005).
7. K. Belfield, X. Ren, E. Van Stryland *et al.*, J. Am. Chem. Soc. **122**, 1217 (2000).
8. K. Schafer, J. Hales, M. Balu *et al.*, J. Photochem. Photobiol. A: **162**, 497 (2004).
9. J.D. Bhawalkar, N.D. Kumar, C.F. Zhao *et al.*, J. of Clin. Laser Med. & Surg. **15**, 201 (1997).
10. S.J. Andrasik, K.D. Belfield, M.V. Bondar *et al.*, Chem. Phys. Chem. **8**, 399 (2007).
11. M. Chalfie, T. Yuan, E. Ghia *et al.*, Science **263**, 802 (1994).
12. I. Gryczynski, G. Piszczek, J.R. Lakowicz *et al.*, J. Photochem. Photobiol. A **150**, 13 (2002).
13. A.R. Holzwarth, J. Wendler, and G.W. Suter, Biophys. J. **51**, 1 (1987).
14. C.C. Corredor and Z.-L. Huang, K.D. Belfield, Advanced Materials (Weinheim, Germany) **18**, 2910 (2006).
15. J. Kawamata, M. Akiba, Y. Inagaki *et al.*, J. Non. Opt. Phys. Mat. **13**, 475 (2004).
16. W. Ma, Y. Wu, J. Han *et al.*, J. Mol. Struc. **752**, 9 (2005).
17. K.D. Belfield, M.V. Bondar, F.E. Hernandez *et al.*, Appl. Opt. **43**, 6339 (2004).
18. K. Belfield, M. Bondar, F. Hernandez *et al.*, J. Phys. Chem. B **111**, 12723 (2007).
19. M.G. Kuzyk, J. Chem. Phys. **119**, 8327 (2003).
20. M.G. Kuzyk, J. Chem. Phys. **125**, 154108 (2006).
21. N. Jarkas, J. McConathy, R.J. Voll *et al.*, J. Med. Chem. **48**, 4254 (2005).
22. M. Galanin and Z. Chizhikova, Pis'ma Zh. Eksp. Teor. Fiz., **4**, 41 (1966).
23. C. Xu and W.W. Webb, J. Opt. Soc. Am. B **13**, 481 (1996).
24. M. Sheik-Bahae, A. Said, T. Wei *et al.*, IEEE Quant. Electron. **26**, 760 (1990).
25. J.R. Lakowicz, *Principles of Fluorescence Spectroscopy* (Kluwer/Plenum, New York, 1999).
26. F. Terenziani, A. Painelli, C. Katan *et al.*, J. Am. Chem. Soc. **128**, 15742 (2006).
27. K. Belfield, M. Bondar, O. Kachkovsky *et al.*, J. Luminescence **126**, 14 (2007).
28. W.L. Peticolas, Ann. Rev. Phys. Chem. **18**, 233 (1967).
29. J. Hales, D. Hagan, E. Van Stryland *et al.*, J. Chem. Phys. **121**, 3152 (2004).
30. K. Ohta, L. Antonov, S. Yamada *et al.*, J. Chem. Phys. **127**, 084504 (2007).
31. B.J. Orr and J.F. Ward, Mol. Phys. **20**, 513 (1971).
32. M.J. Frisch, G.W. Trucks, H.B. Schlegel *et al.*, *GAUSSIAN 03 Revision B.05* (Gaussian, Inc., Pittsburgh, PA, 2003).

НОВІ ФЛУОРЕНОВІ МОЛЕКУЛИ З ЕФЕКТИВНИМ ДВОФОТОННИМ ПОГЛИНАННЯМ ДЛЯ БАГАТОПРОФІЛЬНИХ НЕЛІНІЙНО-ОПТИЧНИХ ЗАСТОСУВАНЬ

М.В. Бондар, О.В. Пржонська, Ц.О. Янес, К.Д. Белфілд

Р е з ю м е

В роботі досліджено лінійні та нелінійно-оптичні властивості нових симетричних флуоренових з'єднань квадрупольного типу: 2,7-біс(4-(фенілтіо)стирил)-9,9-дідецил-9Н-флуорен та 2,7-біс(4-(фенілсульфоніл)стирил)-9,9-дідецил-9Н-флуорен. Показано, що дані молекули характеризуються квантовим виходом флуоресценції (до 100%) та сильними ефектами сольватохромії у збудженому електронному стані. Отримано спектри двофотонного поглинання (ДФП) у широкому спектральному діапазоні 480–880 нм двома незалежними методами (двофотонно-індукована флуоресценція та Z-сканування з відкритою апертурою). Величини перерізів ДФП (з максимальними значеннями до 2000 GM) розраховані чисельно за допомогою алгоритму, який враховує перепоглинання із збуджених електронних станів та процеси вимушеного випромінювання. Високий квантовий вихід флуоресценції, фотохімічна стабільність та відносно високі значення перерізів ДФП роблять дані з'єднання перспективними для широкого кола нелінійно-оптичних застосувань, зокрема, для двофотонної візуалізації біологічних об'єктів.